Spin Labels as Molecular Rulers. The Conformational Analysis of a Model System. 1,4-Didoxylcyclohexane Oriented in a Crystalline Host

Ottmar Rohde, Shui Pong Van, William R. Kester, and O. Hayes Griffith*

Contribution from the Institute of Molecular Biology and Department of Chemistry, University of Oregon, Eugene, Oregon 97403. *Received March 18, 1974*

Abstract: The magnetic interactions between two spin labels can provide information regarding the geometries and distances between binding sites of biomolecules. In order to examine this approach, a single-crystal study was performed on the model compound 1,4-didoxylcyclohexane (1,4-bis(4′,4′-dimethyloxazolidine-*N*-oxyl)cyclohexane) included in the corresponding diamine (1,4-bis(4′,4′-dimethyloxazolidine)cyclohexane). Two conformers of the dinitroxide are trapped in the crystalline host, providing an unusual opportunity to test the information esr can provide about the geometrical arrangement of two spin labels. A detailed analysis of the electron–electron dipolar splittings, the *g*-value anisotropy, and the electron–nuclear hyperfine interactions is presented. From these data the two conformers are shown to be the equatorial–equatorial and the axial–axial chair forms of the trans isomer.

Pairs of spin labels can provide new sensitive molecular rulers for determining distances and geometries in biological systems. Some experiments relevant to this goal have been reported. Notable among these are the extensive studies of dinitroxides in solution and in rigid glasses by Rassat, Rozantsev, Lemaire, and others.[1-3] In addition, the dipolar anisotropy has been examined in this laboratory using single crystals containing nitroxide dimers and dinitroxides.[4,5] These solution and single-crystal studies examined dipolar and exchange interactions and have yielded useful information about molecular dynamics and distances between unpaired spins. To date there has been no analysis of the *g*-value and hyperfine anisotropy of oriented dinitroxides. These data, together with the electron–electron dipolar splittings, can provide a full analysis of the spatial arrangement of two interacting nitroxide spin labels. In order to test this approach, we have chosen the model system 1,4-didoxylcyclohexane I trapped in single crystals of the corresponding diamine II.

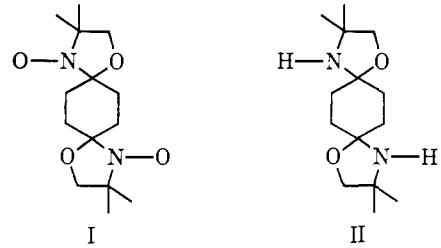

I

II

Normally only one conformational state is expected. However, in this case, two conformers are detected in the same host crystal. The analysis of the data from both conformers provides a stringent test of this approach to determining molecular geometries from the esr data and allows us to distinguish these two conformers from all other major isomers of I shown in Figure 1.

Experimental Section

Preparation of the Host II. The diamine II was prepared from 1,4-cyclohexanedione and 2-amino-2-methyl-1-propanol by the method of Hancock and Cope.[6] It was recrystallized three times from ether:hexane (1:1), mp 102–104° (uncorrected). *Anal.* Calcd: C, 66.11; H, 10.30; N, 11.01. Found: C, 66.41; H, 10.32; N, 10.77.

Preparation of the Dinitroxide I. I was prepared from II by oxidation with *m*-chloroperbenzoic acid in ether solution.[1,7] After recrystallizing three times from benzene:hexane (1:1) large orange platelets were obtained: ir (CCl_4) absence of N–H stretch (3500–3100 cm^{-1}); decomposition point, 172–175° (uncorrected). *Anal.* Calcd: C, 59.14; H, 8.51; N, 9.85. Found: C, 58.94; H, 8.40; N, 9.59.

Growing Crystals of I Trapped in II. Large flat rhombohedrons of II were grown from saturated benzene:hexane (1:1) solutions by slow evaporation. The crystals were stable in air at room temperature. For doping, varying small amounts of dinitroxide I were added to the solution (from I:II = 1:25 to 1:10,000); 1:100 was found to be the optimal ratio. The uptake of I into the host II appeared to be linear with the relative concentration in solution.

Esr Spectra of Polycrystalline Samples. Three different polycrystalline samples were prepared. (a) Doped crystals of II, grown from benzene–hexane at 22°, were powdered and the spectra were recorded at room temperature. (b) Doped crystals of II which had been grown at 22° were dissolved in methanol and recrystallized at −78°. They were removed from the solution, dried at −78°, and brought up to room temperature. After powdering the crystals, the esr spectra were recorded at room temperature. (c) Small amounts of pure dinitroxide I (0.5 mg/ml) were dissolved in EPA (diethyl ether:isopentane:ethanol, 5:5:2 by volume). The rigid glass spectra were recorded at −196°.

Extracting the Dinitroxide I from the Host II. Doped powder (150 mg), I included in II, was dissolved in 2 ml of benzene and neutralized with the exact equivalent of 0.1 *N* aqueous HCl. The benzene layer was washed three times with water and evaporated to dryness. The remaining film of I was dissolved in EPA and frozen in liquid nitrogen to obtain the desired esr spectrum.

Mounting Single Crystals. The mounting of single crystals in a specific orientation is illustrated in Figure 2. After fixing a crystal with one of its faces on the crystal mount, it was rotated about the three axes of the coordinate system (*X*, *Y*, *Z*). The flexible Teflon tip used could easily be bent up or down within a range of ±15° to

(1) A. Rassat, *Pure Appl. Chem.*, **25**, 623 (1971).
(2) E. G. Rozantsev and V. D. Sholle, *Russ. Chem. Rev.*, **40**, 233 (1971).
(3) H. Lemaire, Thesis, Grenoble, 1966.
(4) O. H. Griffith, L. J. Libertini, and G. B. Birrell, *J. Phys. Chem.*, **75**, 3417 (1971).
(5) Z. Ciecierska-Tworek, S. P. Van, and O. H. Griffith, *J. Mol. Struct.*, **16**, 139 (1973).
(6) E. M. Hancock and A. C. Cope, *J. Amer. Chem. Soc.*, **66**, 1738 (1944).
(7) J. F. W. Keana, S. B. Keana, and D. Beetham, *J. Amer. Chem. Soc.*, **89**, 3055 (1967).

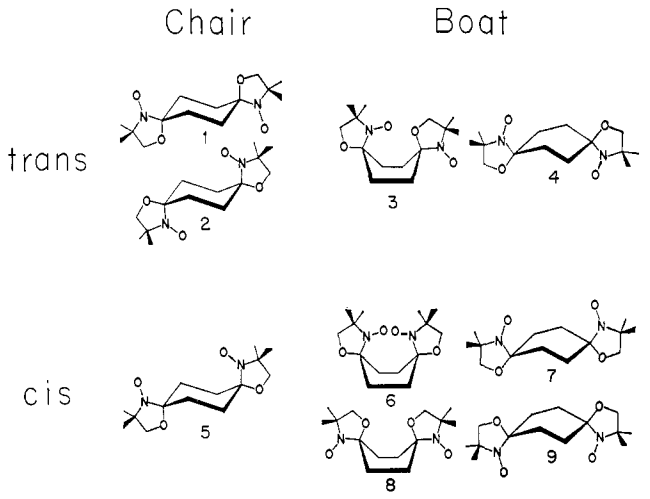

Figure 1. The major structural and conformational isomers of 1,4-didoxylcyclohexane.

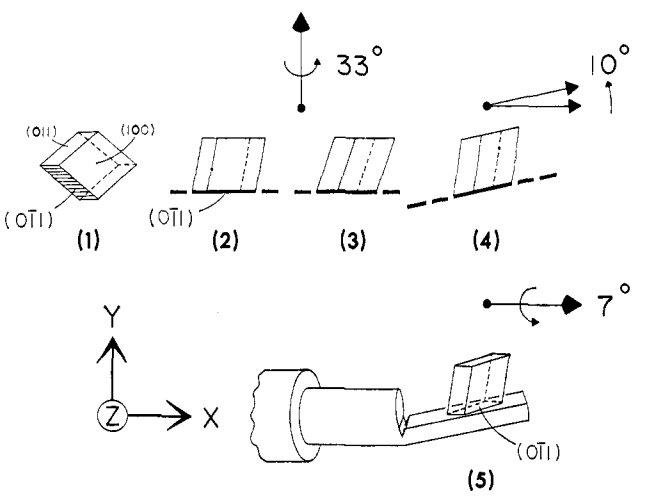

Figure 2. The crystal mounting procedure and the definition of the crystalline coordinate system (X, Y, Z). Esr measurements are performed in the YZ plane. The crystal is oriented by three successive independent rotations on the Teflon mount: (1) typical crystal morphology with the (0$\bar{1}$1) plane shaded, (2) crystal oriented on the mount with the (0$\bar{1}$1) plane in the XZ plane and with the edge between the (0$\bar{1}$1) and (100) planes parallel to the X axis, (3) rotated counterclockwise by 33° about the Y axis, (4) rotated counterclockwise by 10° about the Z axis, (5) crystal and mount after counterclockwise rotation of 7° about the X axis. The X axis is the rotation axis of the mount.

an accuracy of ±1° with the crystal in place. Figure 2 shows how crystals were mounted to obtain data in the YZ plane.

Instrumentation. Esr spectra were recorded on Varian E-Line and E-3 9.5-GHz spectrometers to obtain the splitting data. A Varian V-4502 9.5-GHz spectrometer equipped with a dual sample cavity was used to record the g-value anisotropy. All g-value data were measured relative to di-*tert*-butyl nitroxide in aqueous solution, for which $g_0 = 2.0056$.[8]

Results

X-Ray Crystallographic Data. X-Ray Weissenberg data established that the single crystals of I are monoclinic. The space group is $P2_1/c$ with the a, b, c axes 9.6, 7.5, and 10.6 Å, each accurate to ±0.1 Å, β = 113 ± 1°, and the volume of the unit cell 700 Å^3 (see also Figure 2). The well-developed faces are the (100), (011), (0$\bar{1}$1), and (0$\bar{1}\bar{1}$) Miller planes. The density ρ = 1.16 g/cm^3 was determined by weighing large crystals and measuring their dimensions on a microdensitometer table. From the volume of the unit cell and the crystal density, the number of molecules per unit cell was calculated to be 1.92. Thus, there are two sites per unit cell. These two sites are, according to the space group, magnetically nonequivalent.

Powder and Rigid Glass Spectra. Esr spectra of randomly oriented samples are shown in Figure 3. Figure 3a is the powder spectrum of I trapped in crystals of II grown from benzene–hexane at room temperature. The powder spectrum in Figure 3b was also measured at room temperature, but the crystals were grown from methanol at −78°. Figure 3c is the EPA rigid glass spectrum of I at −196°. Its main splitting is 246 ± 3 G.

Unexpectedly, the powder spectra in Figures 3a and b contain a series of lines which do not appear in Figure 3c. In particular, the two lines with the large splitting of 396 ± 4 G (arrows) in Figure 3a are not seen in the rigid glass spectrum of Figure 3c. Furthermore, the powder and glass spectra can be easily interconverted. When a sample of the dinitroxide I is extracted from the powder, Figure 3a, and is dissolved in EPA and then cooled to −196°, a spectrum almost identical with Figure 3c is obtained where the outermost lines have disappeared. These, therefore, can only arise from an additional conformational state of the dinitroxide I which is present in the host crystals, but not in the EPA rigid glass at low temperatures. The surprising finding that the host preserves two different conformational isomers of I could be supported by preparing powder samples in which the intensity ratios of the two spectral components are different. For example, in Figure 3b the relative population of the additional conformer is smaller than in Figure 3a.

Single-Crystal Spectra. To obtain data of the electron-dipolar splittings and the nuclear hyperfine interactions, esr spectra of oriented single crystals were recorded at least every 2.5° in seven different planes. The smallest measurable step was 0.2°. Three of these planes are the (100) and (011) planes (the faces of the crystal) and the (010) glide plane (which is a mirror plane for the esr data).

A representative spectrum is given in Figure 4. This spectrum consists of four different components, identified by the stick spectra drawn below. The patterns of these components change systematically as the crystal is rotated in the esr cavity. The unit cell contains only two sites, A and B, so that two different spectral components (**1** and **2**) must be attributed to each site, giving a total of four components. Thus two different conformers of I are statistically trapped in each site of the host II. We plotted the dipolar splittings on polar plots which we then assembled to a three-dimensional model. This model yielded important information about the relations between the two conformers and how they are oriented in the host crystal. The YZ crystalline plane is the most important one and will be discussed in detail. Its orientation was derived from the space model. All drawings in this paper (except

(8) G. B. Birrell, S. P. Van, and O. H. Griffith, *J. Amer. Chem. Soc.*, 95, 2451 (1973).

Figures 2 and 8) are presented so that the *YZ* plane is the plane of the paper.

Theoretical Considerations. The Spin Hamiltonian. The spin Hamiltonian of the dinitroxide I trapped in the matrix of the host II is

$$\hat{\mathcal{H}} = \beta\mathbf{H}\cdot\mathbf{g}\cdot\hat{\mathbf{S}} + D(\hat{S}_z^2 - {}^1/_3\hat{\mathbf{S}}^2) + E(\hat{S}_x^2 - \hat{S}_y^2) \quad (1)$$

where **H** is the external magnetic field; β is the Bohr magneton; $\hat{S}_x$, $\hat{S}_y$, $\hat{S}_z$ are the components of the total spin operator $\hat{\mathbf{S}}$; **g** is the electron *g*-value tensor; *D* and *E* are the parameters of the zero-field splitting dipolar tensor. This convenient form of the Hamiltonian can be used in light of the experimental findings. (a) The two doxyl groups of either conformer of I are magnetically equivalent and adequately described by a common *g*-value tensor. (b) The principal axes of the *g*-value tensors nearly coincide with the principal axes of the respective dipolar tensors. In our theoretical treatment we therefore can assume that the *g*-value tensors are diagonal in the respective dipolar coordinate systems. (c) The nuclear hyperfine interactions are only a very small perturbation and can be treated separately.

As the basis functions of the triplet state, we have chosen the functions quantitized in the electron–electron dipolar coordinate system (*x*, *y*, *z*): $|\tau_{+1}\rangle = \alpha\alpha$, $|\tau_0\rangle = (1/\sqrt{2})(\alpha\beta + \beta\alpha)$, $|\tau_{-1}\rangle = \beta\beta$. The direction cosines *l*, *m*, and *n* relate the external magnetic field **H** to the *x*, *y*, *z* coordinates so that $H_x = l|H|$, $H_y = m|H|$, $H_z = n|H|$. The secular determinant[9] of eq 1 is

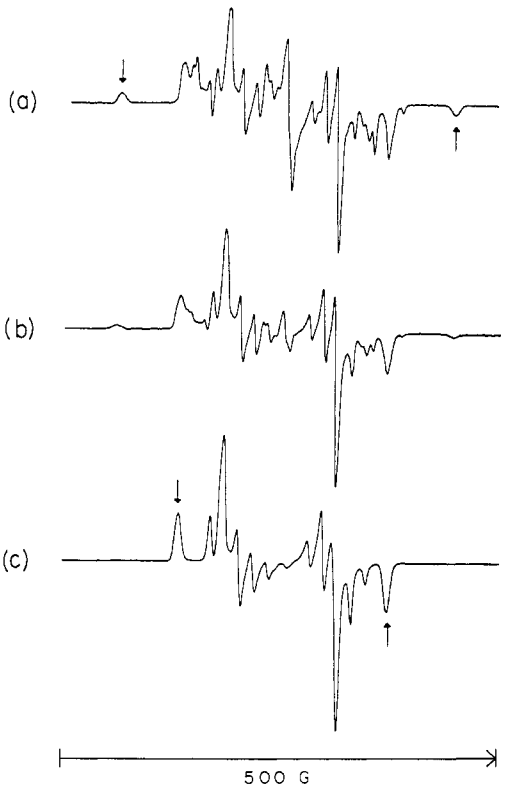

Figure 3. Esr powder and rigid glass spectra showing two conformational states of *trans*-1,4-didoxylcyclohexane. (a) Room-temperature powder spectrum of I trapped in crystals of II grown from benzene–hexane at 20° and (b) trapped in crystals grown from methanol at −78°. (c) EPA rigid glass spectrum of I at −196°.

$$\begin{array}{c|ccc} & |\tau_{+1}\rangle & |\tau_0\rangle & |\tau_{-1}\rangle \\ \langle\tau_{+1}| & {}^1/_3D - g_{zz}\beta Hn - W & 2^{-1/2}\beta H(g_{xx}l - ig_{yy}m) & E \\ \langle\tau_0| & 2^{-1/2}\beta H(g_{xx}l + ig_{yy}m) & -{}^2/_3D - W & 2^{-1/2}\beta H(g_{xx}l - ig_{yy}m) \\ \langle\tau_{-1}| & E & 2^{-1/2}\beta H(g_{xx}l + ig_{yy}m) & {}^1/_3D + g_{zz}\beta Hn - W \end{array} \quad (2)$$

Expansion of eq 2 yields

$$\left(W - \frac{D}{3} + E\right)\left(W - \frac{D}{3} - E\right)\left(W + \frac{2D}{3}\right) - (g\beta H)^2\left[\left(W + \frac{2D}{3}\right) - D(G_x^2 + G_y^2) + E(G_x^2 - G_y^2)\right] = 0 \quad (3)$$

with

$$G_x^2 = \frac{g_{xx}^2 l^2}{g^2},\ G_y^2 = \frac{g_{yy}^2 m^2}{g^2},\ G_z^2 = \frac{g_{zz}^2 n^2}{g^2}$$

and

$$g^2 = g_{xx}^2 l^2 + g_{yy}^2 m^2 + g_{zz}^2 n^2 \quad (4)$$

We solved the cubic eq 3 numerically for varying values of *l*, *m*, and *n* to give the two magnetic field strengths, H_1 and H_2, at which the transitions $|\tau_{-1}\rangle \rightarrow |\tau_0\rangle$ and $|\tau_0\rangle \rightarrow |\tau_{+1}\rangle$ occur. The apparent dipolar splitting *d* (in gauss) of the corresponding esr spectra is given by $|H_2 - H_1|$. The apparent *g* value, $\bar{g}$, was calculated from the average field strength $\bar{H} = (H_1 + H_2)/2$ and and the relation $h\nu = \bar{g}\beta\bar{H}$. All calculations were performed in reference to a frequency of 9.5 GHz. We found that the dipolar splittings are equally well described by the familiar first-order solution

$$d(\theta,\phi) = |D(3\cos^2\theta - 1) + E(3\sin^2\theta\cos 2\phi)| \quad (5)$$

in which **H** is related to the dipolar coordinates by the spherical coordinates θ and ϕ.[5,10] Even for large dipolar interactions the values calculated from eq 5 are nearly identical with those obtained from eq 3.

Obtaining Self-Consistent Quantities from the Experiment. In our case the dipolar interactions are sufficiently large that the experimental *g* values have to be corrected according to the method used by Hutchison and Mangum.[11] The self-consistent quantities g_{xx}, g_{yy}, g_{zz}, *D*, and *E* can be calculated from the experimentally measured quantities g_{xx}, g_{yy}, $\bar{g}_{zz}$, $\bar{D}$, $\bar{E}$ using the following simple expressions.

$$g_{xx} = \bar{g}_{xx} - \delta g = \bar{g}_{xx}\left(1 - \frac{(\bar{D} + \bar{E})^2}{8\bar{H}^2}\right) \quad (6)$$

$$g_{yy} = \bar{g}_{yy} - \delta g = \bar{g}_{yy}\left(1 - \frac{(\bar{D} - \bar{E})^2}{8\bar{H}^2}\right) \quad (7)$$

$$g_{zz} = \bar{g}_{zz} - \delta g = \bar{g}_{zz}\left(1 - \frac{\bar{E}^2}{2\bar{H}^2}\right) \quad (8)$$

(9) S. P. McGlynn, T. Azumi, and M. Kinoshita, "Molecular Spectroscopy of the Triplet State," Prentice-Hall, Englewood Cliffs, N. J., 1969, pp 350–368.

(10) E. B. Wilson, Jr., J. C. Decius, and P. C. Cross, "Molecular Vibrations," McGraw-Hill, New York, N. Y., 1955, pp 285–286.

(11) C. A. Hutchison, Jr., and B. W. Mangum, *J. Chem. Phys.*, 34, 908 (1961).

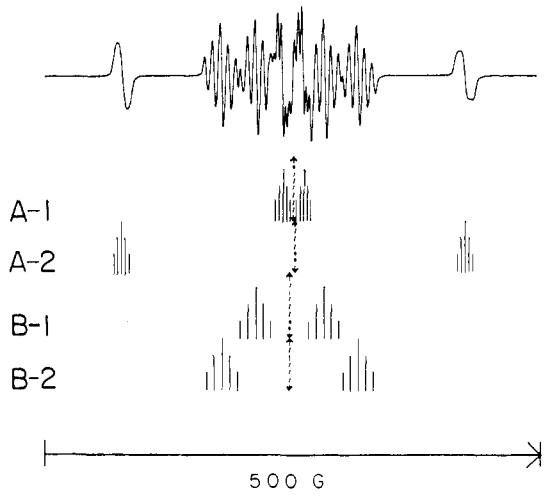

Figure 4. Esr spectrum of dinitroxide I trapped in a single crystal of the corresponding diamine II. The four different sets of esr signals are attributed to two conformational isomers (**1** and **2**) of dinitroxide I occupying two magnetically nonequivalent sites (A and B) in the host crystal.

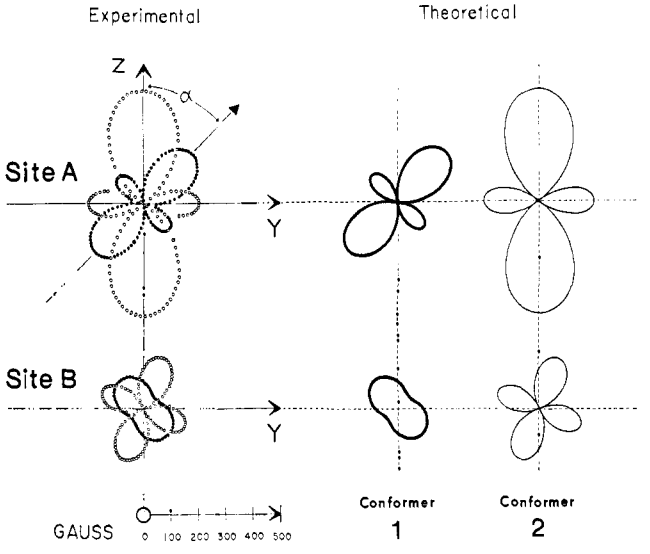

Figure 5. Polar plots of the dipolar splitting in the *YZ* plane. The experimental data of the two magnetic nonequivalent sites A and B are shown separately. The theoretical plots are calculated by using the parameters in Table I.

Equations 6–8 are convenient simplifications of eq 10.12 and 10.14 in ref 9 whereby we set $\bar{H}$ at 3390 G when using a frequency of 9.5 GHz. The differences δg between the self-consistent and apparent g values are small and they are given accurately by these equations. For the dinitroxide I, we found that the differences between the measured parameters $\bar{D}$ and $\bar{E}$ and the corresponding self-consistent values D and E are negligible, thus we set $D = \bar{D}$ and $E = \bar{E}$.

The Zero-Field Dipolar Splittings. The most accurate of our measurements are the electron–electron dipolar splittings. The dipolar splitting d of each of the four spectral components is given by the distance between the midpoints of the two five-line patterns. Each component has a dipolar coordinate system (x, y, z) where, according to eq 5, the maximum splitting $|2D|$ defines the z axis, $|-D + 3E|$ the x axis, and $|-D - 3E|$ the y axis. Polar plots of these dipolar

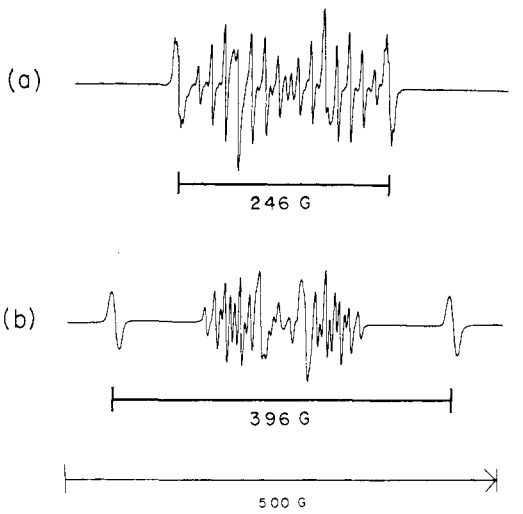

Figure 6. Esr single-crystal spectra at the principal orientations: (a) with the magnetic field along the dipolar z axis of conformer **1** (the molecular Z_1 axis) and (b) with the magnetic field along the dipolar z axis of conformer **2** (the molecular Z_2 axis).

splittings recorded in the *YZ* plane are shown in the left column of Figure 5. Two curves, denoted by solid and open circles, are obtained for each site. These two curves arise from two different conformers of the dinitroxide I trapped in the same site. The data for site A and B are plotted separately but were obtained simultaneously. In Figure 5 the data for site A are of special interest because these plots exhibit the maximum splitting for both conformers. The maximum splitting of conformer **2** occurs along the crystalline Z axis; the maximum splitting of conformer **1** occurs at the angle $\alpha = 44.5 \pm 1.0°$ from the Z axis in the *YZ* plane. The two esr spectra taken at these two special orientations are shown in Figure 6. There is substantial overlap of spectral components from sites A and B, but the outermost lines are clearly visible in Figure 6, yielding $2D = \pm 246 \pm 3$ G for conformer **1** and $2D = \pm 396 \pm 4$ G for conformer **2**. These values are identical with those measured from the powder spectra. Measurements in planes normal to the *YZ* plane indicate that the parameter E is $\mp 2.2 \pm 0.5$ G for conformer **1** and $\mp 2.0 \pm 0.5$ G for conformer **2**. These values are also consistent with the powder spectra. In both cases, E is so small that the dipolar tensors can be taken as axially symmetric about the respective dipolar z axis. The dipolar coordinate system of each spectral component is related to the X, Y, Z crystalline coordinate system by a set of three Eulerian angles[10] Φ, Θ, χ. Those angles are listed in Table I together with the respective values of D and E.

Table I. Parameters of the Zero-Field Dipolar Splittings[a]

Spectral component	$2D$	E	Φ	Θ	χ
A-1	± 246	∓ 2.2	0	44.5	90
A-2	± 396	∓ 2.0	0	0	55
B-1	± 246	∓ 2.2	−36	−73.5	−18
B-2	± 390	∓ 2.0	−79	−107	−49

[a] Units: D, G; E, G; Φ, Θ, and χ, deg. Φ, Θ, and χ are the Eulerian angles relating the four dipolar coordinate systems (two for each site) to the X, Y, Z crystalline coordinate system. The estimated accuracies are $\pm 1\%$ for $2D$, $\pm 20\%$ for E, and $\pm 2°$ for Φ, Θ, and χ.

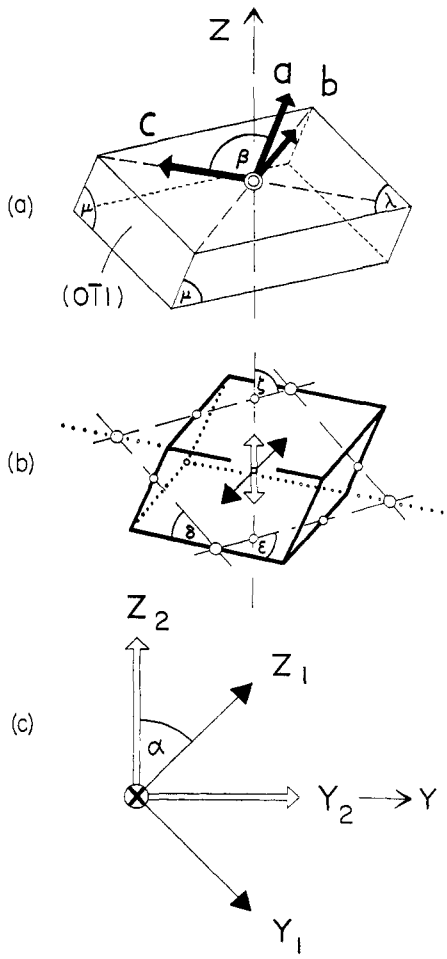

Figure 7. Spacial orientation of the molecular coordinates in the host crystal. (a) Crystal morphology of the host compound II showing the crystalline axes *a*, *b*, *c*. The macroscopic face angles λ and μ are 79.3 and 71.2°, respectively, each accurate to ±0.5°. (b) Unit cell with the crystalline *YZ* plane indicated by four dashed lines. The dark and light arrows represent the dipolar *z* axes of the two conformers **1** and **2**, trapped in site A. δ, ϵ, and ζ are obtained from the space model of the dipolar graphs and are 49.0, 48.5, and 71.5°, respectively (each accurate to ±2°). (c) The two molecular coordinate systems (X_1, Y_1, Z_1) and (X_2, Y_2, Z_2); α = 44.5 ± 1.0°.

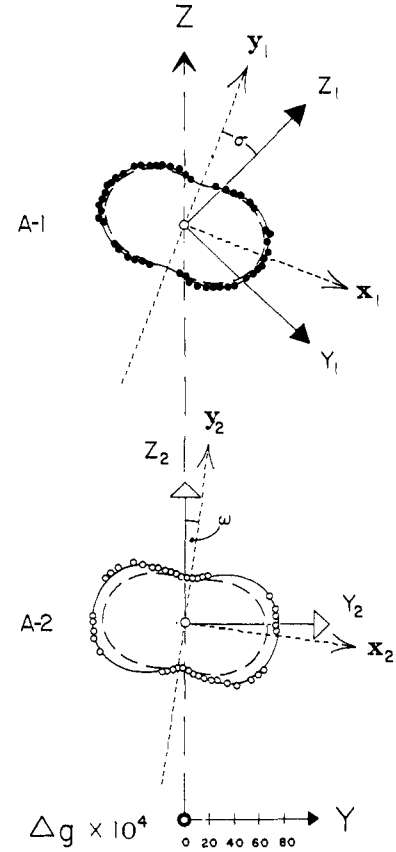

Figure 8. Polar plots of the *g* values in the *YZ* plane. Only the data of site A are shown. The increment $\Delta g = (g - 2.0020) \times 10^4$ is plotted *vs.* angle, so that the *g* value 2.0020 forms the center of the plots and the reading 80 corresponds to a *g* value of 2.0100. Solid and open circles are experimental data. The solid lines are the theoretical curves from eq 3. The dashed lines are calculated from a first-order treatment. Note that the principal axes of the *g*-value anisotropy (y_1 and y_2) differ from the dipolar Z_1 and Z_2 axes by the angles σ and ω of 23.5 and 6°, each accurate to ±2°, respectively.

The theoretical curves in Figure 5 have been calculated by applying the experimental parameters in Table I to a first-order solution of eq 2.

Figures 7a and 7b illustrate how the esr data obtained from conformer **1** and **2** in site A are spatially related to the crystal morphology and the unit cell of the host. We found it convenient to define two molecular coordinate systems X_1, Y_1, Z_1, and X_2, Y_2, Z_2 as shown in Figure 7c. The molecular Z_1 and Z_2 axes lie along the dipolar *z* axes of the respective conformers; the X_1 and X_2 axes are chosen to coincide with the crystalline *X* axis. The Y_1 and Y_2 axes therefore lie in the *YZ* plane, perpendicular to the Z_1 and Z_2 axes, respectively. These two coordinate systems will be used when discussing the *A* and *g* value data. As the asymmetry of the dipolar tensor between the *x* and *y* directions, *E*, is so small, these coordinates can then be used as the dipolar coordinates as well.

The *g*-Value Anisotropy. The principal axes of the *A* and *g* value tensors of a mononitroxide coincide and together define the geometrical *x*, *y*, *z* axes of the nitroxide group. In order to obtain information about the orientation of the doxyl groups in I, we have recorded the *g*-value anisotropy of both conformers of I in the crystalline *YZ* plane and the molecular X_1Y_1 and X_2Y_2 planes as defined in Figure 7. The two polar plots in Figure 8 show the experimental *g*-value anisotropy measured in the *YZ* plane. The upper plot (A-1) contains the experimental data of conformer **1** in site A. The lower plot (A-2) presents the data of conformer **2** in site A.

We have found that the *YZ* plane is a mirror plane of the *g*-value anisotropy of both conformers. Two principal values are found in this plane in directions nearly along the Y_1 and Z_1 axes (or Y_2 and Z_2 axes, respectively). These directions define the nitroxide x_1 and y_1 (or x_2 and y_2) axes. This is the standard convention where the x_1 axis is along the N–O bond, the z_1 axis is parallel to the π orbital associated with the unpaired electron, and the y_1 axis is perpendicular to both the π orbital and the N–O bond.

In our case the dipolar splittings are sufficiently large so that the self-consistent principal *g* values must be calculated from the experimental data using eq 6–8. Table II lists the experimentally obtained principal values $\bar{g}$, the correction from δg, the final self-consistent value *g*, and the principal values of the *mononitroxide*

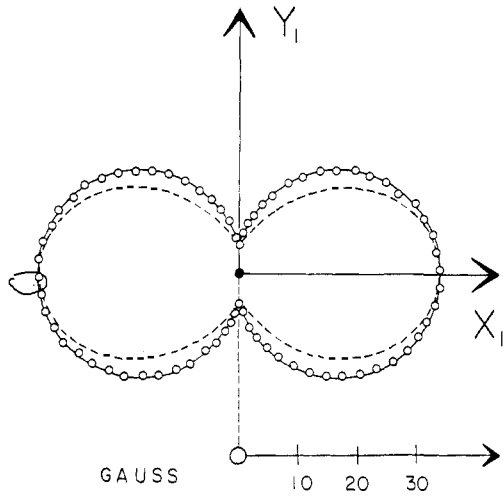

Figure 9. Polar plot of the hyperfine splittings from site A in the molecular X_1Y_1 plane, perpendicular to the crystalline YZ plane. Open circles are experimental data obtained from the spectral component A-1. Dashed and solid lines are plots of eq 9 and 10, respectively.

Table II. The Principal g Values[a]

Conformer	Direction	$\bar{g}$	δg	g	g(2DP)[b]
1	g_{xx}	2.0025	0.0003	2.0022	2.0022
	g_{yy}	2.0093	0.0003	2.0090	2.0088
	g_{zz}	~2.0058	0	~2.0058	2.0058
2	g_{xx}	2.0027	0.0008	2.0019	2.0022
	g_{yy}	2.0096	0.0008	2.0088	2.0088
	g_{zz}	2.0057	0	2.0057	2.0058

[a] The estimated accuracy of all g values is ±0.0003. [b] Values of g for 2-doxylpropane (2DP) from ref 12.

2-doxylpropane for comparison. These calculations were performed under the assumption that the principal directions of the g-value anisotropy coincide with the respective molecular coordinates. We refer to the principal values as g_{xx}, g_{yy}, g_{zz} where x, y, z are the directions of the respective molecular coordinates X_1, Y_1, Z_1 (and X_2, Y_2, Z_2). The representation of the principal directions in the molecular coordinates X_1, Y_1, Z_1 (and X_2, Y_2, Z_2) is related to the representation in nitroxide coordinates x, y, z by the permutation $g_{zz} \rightarrow g_{xx}$, $g_{yy} \rightarrow g_{zz}$, $g_{xx} \rightarrow g_{yy}$. Therefore, for example, the values g_{zz} in Table II correspond to g_{yy}, when using the convention employed for mononitroxides.

In Figure 8 we compare the apparent experimental data to two different theoretical solutions. The solid lines were obtained from the numerical solution of the secular eq 2 using the self-consistent principal values g obtained from eq 6–8. The dashed curves were calculated from the first-order solution of the spin Hamiltonian. The difference between the solid and the dashed curves arises from the dipolar interactions. According to eq 6–8, this difference is approximately proportional to the square of D or of E, depending on the principal direction being considered.

From the data in Figure 8 and those taken in the X_1Y_1 and X_2Y_2 planes we infer the following. (a) Both doxyl groups in either conformer of I are magnetically equivalent and adequately described by a common g-value tensor. (b) In either conformer the two N–O groups have common geometrical axes. (We refer to these nitroxide axes as the x_1, y_1, z_1 axes for conformer **1** and x_2, y_2, z_2 axes for conformer **2**.) The z_1 and the z_2 axes are both perpendicular to the YZ plane. (c) The nitroxide coordinates are different from the respective molecular coordinates only by the small angles σ and ω in the YZ plane. This justifies the assumptions made in eq 2.

The Hyperfine Structure. The symmetry properties of both conformers are even more obvious from the nuclear hyperfine interactions. Each of the esr spectral components consists of two groups of five equally spaced lines with the relative intensities of 1:2:3:2:1. The spacing between adjacent lines is half the spacing expected from a mononitroxide. This pattern is maintained even at those particular orientations where the dipolar splittings are zero. This indicates that the two nitrogen atoms are equivalent and that the magnitude of the exchange integral J is much greater than the hyperfine interactions. Surprisingly, the same hyperfine splittings are observed for both conformers in a given site. The stick spectra in Figure 4 emphasize that the hyperfine splittings of the spectral components A-1 and A-2 are identical as are the splittings of the components B-1 and B-2. We observe the maximum hyperfine splitting of the spectral components A-1 and A-2 (conformer **1** and **2** in site A) along the X axis. Figure 9 presents the data from the spectral component A-1 in the molecular X_1Y_1 plane perpendicular to the YZ plane. The principal values (multiplied by a factor of 2) are listed in Table III in comparison to the values of

Table III. Parameters of the Nuclear Hyperfine Interactions[a]

	A_{xx}	A_{yy}	A_{zz}
Conformer **1**	~5	~5	33.0 ± 0.5
Conformer **2**	~5	~5	33.0 ± 0.5
2DP[b]	5.9	5.4	32.9

[a] Units, G. [b] Splitting between adjacent lines of 2-doxylpropane.

the mononitroxide, 2-doxylpropane. In Figure 9 we compare the experimental data (open circles), multiplied by two, to the familiar theoretical expressions used for mononitroxides.[12,13]

$$A(\theta,\phi) = A_{xx} \sin^2\theta \cos^2\phi + A_{yy} \sin^2\theta \sin^2\phi + A_{zz} \cos^2\theta \quad (9)$$

$$A(\theta,\phi) = \{A_{xx}^2 \sin^2\theta \cos^2\phi + A_{yy}^2 \sin^2\theta \sin^2\phi + A_{zz}^2 \cos^2\theta\}^{1/2} \quad (10)$$

Equations 9 and 10 are referred to as the high-field ($H \gg H_{hf}$) and the intermediate-field ($H \simeq H_{hf}$) solutions, where H is the external magnetic field and H_{hf} is the field caused by the electron at the nucleus.[13]

The solid line in Figure 9 was calculated from eq 10; the dashed curve gives the results from eq 9. We note that eq 10 with the principal values of Table III provides a good description of the experimental hyperfine data at all directions of the crystal in the magnetic field.[12]

Discussion

The esr spectra of the powder samples consist of two

(12) P. Jost, L. J. Libertini, V. C. Hebert, and O. H. Griffith, *J. Mol. Biol.*, **59**, 77 (1971).
(13) L. J. Libertini and O. H. Griffith, *J. Chem. Phys.*, 53, 1359 (1970).

interconvertible components. Only one of these components is seen in the EPA rigid glass spectrum. This reflects the fact that two different conformational isomers of I are trapped in the crystalline host, only one of which is present in the EPA glass at low temperatures. The dipolar splittings, $|2D|$, readily measured from the outermost lines of each spectral component, are related to the intramolecular distance between the N–O groups of the respective conformers. According to the familiar point dipole approximation, the distance between the unpaired spins, r, is given by[14]

$$r = \left[\frac{5.56 \times 10^4}{|2D|}\right]^{1/3} \qquad (11)$$

where r is measured in ångstroms and D in units of gauss.

From eq 11 the experimental values $|2D| = 246$ and 396 G correspond to $r = 6.09$ and 5.20 Å, respectively. We find from measurements on molecular models that the intramolecular distance between the midpoints of the N–O bonds are approximately 6.2 Å in the e,e chair and 4.7 Å in the a,a chair of the trans isomer (conformers **1** and **2** in Figure 1). Thus, these two conformers are consistent with the powder spectra and the EPA rigid glass spectrum. These conclusions agree with measurements by Rassat, who observed the splitting of 250 G in a rigid glass spectrum of I and noted that this value is consistent with the e,e form of the trans-chair (conformer **1**).[1] The magnitude of the dipolar splitting, $|2D|$, alone, however, is not sufficient to distinguish conformers **1** and **2** from all the possible isomers shown in Figure 1. Isomers **3**, **5**, and **6** are easily eliminated, but isomers **1**, **8**, and **9** have similar values of r, as have isomers **2**, **4**, and **7**. Positive identification can be made from the single-crystal g value and hyperfine data.

Each single-crystal spectrum is composed of four different esr spectral components, whereas the unit cell of the host II contains only two magnetically nonequivalent sites. In the esr experiment the two sites are related to each other by the (101) mirror plane (the plane common to the a and c crystalline axes). In principle there are two different ways to attribute two out of four spectral components to each of those sites. Fortunately, our esr data clearly indicate which components are associated with the same site. Two independent criteria classify the four spectral components. (1) According to the graphs of the dipolar splittings (Figure 5 and Table I), the four spectral components appear in two pairs, **1** and **2**, each pair characterized by common values of D and E. Each pair is arranged symmetrically with respect to the (010) mirror plane and represents one conformer. (2) Each single-crystal spectrum can be grouped as well into two pairs (A and B) of spectral components with identical hyperfine structure. Spectral components with identical hyperfine structure clearly belong together in the same site. We can interpret our esr data only when attributing the components A-**1** and A-**2** to site A and the components B-**1** and B-**2** to site B. Our data exclude the alternative possible arrangement, namely A-**1**, B-**2** associated in one site and B-**1**, A-**2** in the other.

(14) P. Jost and O. H. Griffith in "Methods in Pharmacology," Vol. II, C. Chignell, Ed., Appleton-Century-Crofts, New York, N. Y., 1971, p 242.

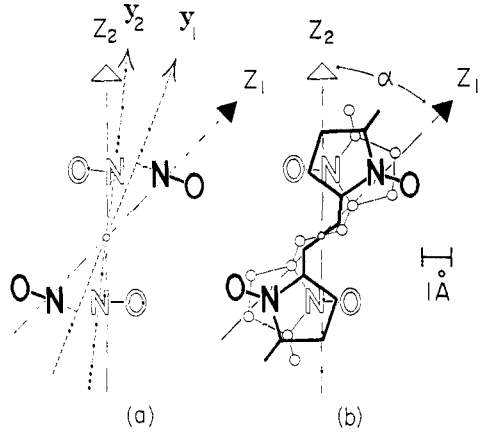

Figure 10. Equatorial–equatorial (light) and axial–axial (dark) *trans*-1,4-didoxylcyclohexane alternatively substituting the same site in the single crystal of the corresponding diamine II. (a) Relative positions of the nitroxide groups as derived from the molecular dimensions and the orientations of the principal axes Z_1, Z_2, y_1, and y_2. (b) Projection formula of the two conformers. Note that the dipolar Z_1 and Z_2 axes intersect the N–O bonds at about one-fourth the bond length from the nitrogen atoms.

The hyperfine and g-value data enabled us to distinguish the conformers **1** and **2** from all the other possible isomers shown in Figure 1. The hyperfine data indicate that the π orbitals at the nitrogen atoms are parallel to each other and perpendicular to a plane common to both conformers (the YZ plane). This is not compatible with the boat forms **4**, **7**, and **9** (and their twisted derivatives) in which the π orbitals are tilted with respect to each other. The hyperfine data are sensitive to the direction of the π orbitals and clearly show that the nitroxide z axes lie along the crystalline X axis, as defined in Figure 2. From the g-value data we note that the two nitroxide groups in either conformer of I have common geometrical axes x, y, z. They are therefore either parallel or related to each other by a rotation of 180° about one of those principal axes. *Only the equatorial–equatorial and the axial–axial forms of the trans-chair (conformers* **1** *and* **2***) obey these conditions. Therefore, we conclude, crystals of* II *include the dinitroxide* I *in both conformers simultaneously.*

Furthermore, our single-crystal data uniquely determine how the two guest molecules are oriented in the host crystal. Since the host molecule has a center of inversion just as the two conformers of I, all three must possess a common center of symmetry at the same site. Figure 10 shows the projection formulas of conformers **1** and **2** drawn from standard bond lengths and angles and X-ray crystallographic data from other nitroxides.[15–18] They are arranged with a common center

(15) L. J. Berliner, *Acta Crystallogr., Sect. B*, **26** 1198 (1970).

(16) A. Capiomont, B. Chion, and J. Lajzérowicz, *Acta Crystallogr., Sect. B*, 27, 322 (1971).

(17) W. Turley and F. P. Boer, *Acta Crystallogr., Sect. B*, **28**, 1641 (1972).

(18) During the preparation of this manuscript, we became aware of the X-ray structure determination of single crystals of I by W. B. Gleason, *Acta Crystallogr., Sect. B*, **29**, 2959 (1973). He reports that the conformer present in pure crystals of I is the equatorial–equatorial form of the trans-chair (conformer **1**). No other conformers of I are observed. Thus, although the molecular environments are different, the X-ray crystallographic data are consistent with the present study. The projection formula of conformer **1** (Figure 10b, dark line), which we have drawn from standard bond lengths and angles, is essentially the same as that observed by Gleason.

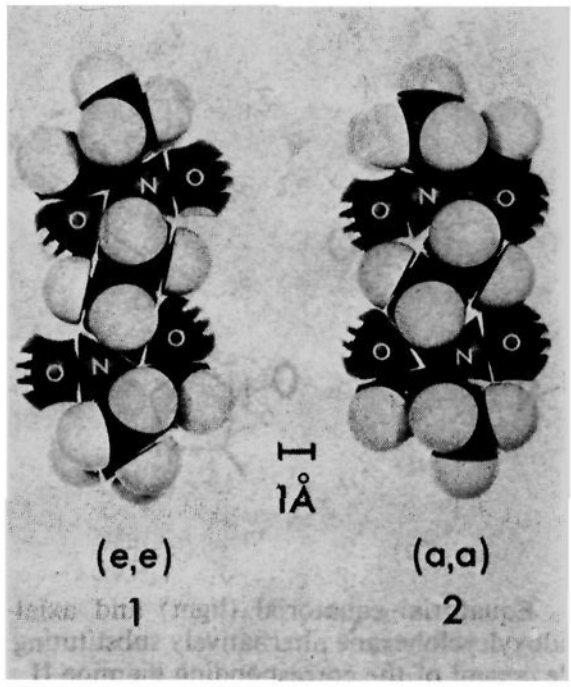

Figure 11. The space-filling models of conformers **1** and **2**.

of symmetry, so that the Z_1 and Z_2 axes interconnect the respective N–O bonds, and the axes of the nitroxide groups are the principal directions found from the hyperfine and *g*-value data. Figure 10, then, illustrates how the two conformers alternatively substitute in the same site of the host. We note that the guest molecule II cannot flip from one conformational state to the other after being trapped in the host crystal.

Figure 11 presents the Pauling–Corey–Kolton molecular models of conformers **1** and **2**. We have oriented the two molecules visually so that they would occupy approximately the same site. When superimposed by horizontal translation, the orientation of the two molecules relative to each other is nearly the same as in Figure 10, which was derived solely from the esr data.

In Figure 10 it was necessary to let the dipolar *z* axes (the molecular Z_1 and Z_2 axes) intersect the N–O bonds at approximately one-fourth the bond length from the nitrogen atoms. If the point of intersection were elsewhere, each of the molecules would have to be rotated by an angle ξ about the *X* axis normal to the plane of the paper in order to maintain the experimental angle of $\alpha = 44.5°$. At the same time the y_1 and y_2 axes would be rotated relative to each other by 2ξ. However, the relative orientation of these two axes is known to an accuracy of $\pm 3°$. Similar conclusions can be drawn from the molecular models in Figure 11. From Figure 11 we have measured $\alpha = 42°$, assuming that the dipolar *z* axes intersect the N–O bonds at one-fourth the bond length from the nitrogen atoms. This value is surprisingly close to the experimentally measured angle $\alpha = 44.5°$. If the point of intersection were the middle of the bond, α would be 54°; likewise, α becomes 28° when the dipolar *z* axes intersect directly at the nitrogen atoms.

In summary, when using spin labels as molecular rulers, three sources of information are available: the electron–electron dipolar splittings, the *g*-value anisotropy, and the electron–nuclear hyperfine interactions. Each has its advantages and limitations. The dipolar splitting, $|2D|$, obtained easily from esr powder spectra, provides a direct measure of the distance between the N–O groups. The dipolar interactions are highly anisotropic, so that the direction of the vector connecting the two N–O groups can be obtained from the single-crystal data with high precision. In our study the anisotropy of the dipolar splittings was also very useful in distinguishing and identifying different spectral components. The dipolar data, however, usually do not provide information about the relative orientation of two interacting spin labels. We have obtained this information from the single-crystal hyperfine and *g*-value data. In an ideal case the *g*-value anisotropy alone can determine the orientations of nitroxide groups. In spite of extensive spectral overlap the *g*-value data collected were sufficient to determine all principal directions of the *g*-value anisotropy. These data, together with the dipolar splittings, positively identify conformers **1** and **2** and rule out all other isomers in Figure 1. The electron-nuclear hyperfine data confirm this assignment. Although they do not distinguish between the nitroxide *x* and *y* coordinates, the hyperfine data identify the nitroxide *z* axis with higher precision than do the *g*-value data. From the hyperfine data alone, we could not distinguish all possible isomers of I, but these data were useful in deriving important symmetry relations between the nitroxide groups.

Acknowledgment. We are pleased to acknowledge helpful discussions with Dr. Brian Matthews and Dee Brightman. We gratefully acknowledge support by U. S. Public Health Service Grant CA10337 from the National Cancer Institute. O. R. wishes to sincerely thank the Fulbright-Hays Fellowship Program for financial support and Dr. U. Littmann, B.-B. Godesberg, and L. McNally, San Francisco, Calif., for their encouragement. O. H. G. acknowledges general support by C.D.A. Grant 1 KO4 CA23359 from the National Cancer Institute.